

The Application of Series Elastic Actuators in the Hydraulic Ankle-Foot Orthosis

A THESIS
SUBMITTED TO THE FACULTY OF
UNIVERSITY OF MINNESOTA
BY

JEONG YONG KIM

IN PARTIAL FULFILLMENT OF THE REQUIREMENTS
FOR THE DEGREE OF
MASTER OF SCIENCE

ADVISOR: WILLIAM DURFEE

SEPTEMBER 2017

© 2017 Jeong Yong Kim
All rights reserved.

Abstract

Advances in wearable technology have been trending toward more powerful and lightweight devices. A type of wearable device that fits into this trend is the Ankle-Foot Orthosis (AFO), which is a device that restrains or strengthens the movement of an ankle to assist the user during gait. A powered AFO uses an actuator and power supply to add positive power to the ankle but becomes heavier as the power output increases. To address the high power requirement and the need for a lightweight design, a hydraulic series elastic actuator (HSEA) was explored to determine whether it could be used to design a lightweight powered AFO that meets the high peak power demand of gait. Hydraulic power has excellent power density and the ability to lower the weight of the AFO at the ankle by separating the power supply from the actuator by a hose. In addition, a series elastic actuator can take advantages of the high-peak and low-average power profile of ankle gait to store energy and release it during the push off stage of gait. The parameters required for the series elastic actuator were calculated and validated using simulation. The velocity and torque of a gait pattern that requires 250W of peak power were able to be tracked using a 95W power supply. The actuator and power supply overall weight was reduced by 20% with the weight of the actuator at the ankle less than 0.5 kg. A novel design of a HSEA with a clutch capability is proposed for future AFO applications.

Table of Contents

| | |
|--|-----|
| List of Tables | iii |
| List of Figures | iv |
| 1.0 Introduction..... | 1 |
| 1.1 Background and Motivation | 1 |
| 1.2 Ankle Dynamics of Human Gait..... | 3 |
| 1.3 Series Elastic Actuators (SEA) | 5 |
| 1.4 Hydraulic Power | 6 |
| 1.5 Prior art | 6 |
| 1.6 Project Objective..... | 8 |
| 2.0 HAFO Design using SEA | 8 |
| 2.1 Direct Drive HAFO Design | 8 |
| 2.2 Designing a Hydraulic SEA..... | 10 |
| 2.2.1 Comparison of different elastic components..... | 10 |
| 2.2.2 Spring Constant and Power Amplification | 13 |
| 2.2.3 Gait Simulation | 16 |
| 2.3 Conceptual Design of a Hydraulic Series Elastic Actuator (HSEA) | 21 |
| 2.3.1 Design Requirements | 21 |
| 2.3.2 Hydraulic Series Elastic Actuator (HSEA)..... | 22 |
| 2.4 Weight Evaluation | 25 |
| 3.0 Discussion..... | 26 |
| References..... | 28 |
| Appendix..... | 30 |
| A. Preliminary Experimental Analysis of a Novel Hydraulic SEA Actuator | 30 |

List of Tables

Table 1. Design requirements of direct drive HAFO 9

Table 2. Component weight in kilograms of five systems 25

List of Figures

| | |
|---|----|
| Figure 1. Multi-joint wearables in the market. The Rewalk Personal 6.0 (left) and Lokomat (right) | 1 |
| Figure 2. Hydraulic Ankle-Foot Orthosis (HAFO) developed by University of Minnesota.. | 3 |
| Figure 3. The human gait cycle..... | 4 |
| Figure 4. The kinematics and kinetics of the human gait cycle [5]..... | 5 |
| Figure 5. Components of a series elastic actuator..... | 6 |
| Figure 6. AFO using SEA by MIT (left) and powered AFO using PMA by University of Michigan (right)..... | 7 |
| Figure 7. Powered AFO using robotic tendon technology..... | 8 |
| Figure 8. Direct drive HAFO. Hydraulic power supply located at the waist (left)and actuator at ankle (right)..... | 9 |
| Figure 9. Configurations of the systems simulated. All configurations are closed-circuit hydraulic systems.System 1 (top): Direct drive, System 2 (middle): Series elastic actuator with spring, System 3 (bottom):Series elastic actuator with accumulator | 11 |
| Figure 10. Normalized velocity of mass (a) with different spring constants and (b) of the three different systems. | 12 |
| Figure 11. Model of series elastic actuator. | 13 |
| Figure 12. Optimization of spring constant by maximizing power amplification. | 15 |
| Figure 13. Spring constant versus pulley radius. | 16 |
| Figure 14. Block diagram of simulation..... | 17 |
| Figure 15. Model of powered AFO using SEA..... | 17 |
| Figure 16. Position tracking of 95W and 250W direct drive systems during simulated gait. | 18 |
| Figure 17. Power required by gait versus power generated by the DD systems..... | 19 |
| Figure 18. Ankle position tracking comparison of DD and SEA 95W systems. | 20 |
| Figure 19. Power required by gait and power generated by DD and SEA..... | 21 |
| Figure 20. Diagram of design requirements categorized into specific demands..... | 22 |
| Figure 21. HSEA design in (a) retracted and (b) extended positions..... | 23 |
| Figure 22. Simplified cross-section of HSEA and related parameters..... | 23 |

| | |
|--|----|
| Figure 23. Cylinder piston movements during push off. (a) spring is compressed and (b) energy stored is released. | 24 |
| Figure 24. Weight distribution of different systems between ankle and waist. | 26 |
| Figure 25. Apparatus. | 30 |
| Figure 26. Series elastic actuator bench test setup. | 31 |
| Figure 27. Selection of spring constant for bench test. | 32 |
| Figure 28. The position (a) and velocity (b) of input cylinder and spring end. The deformation (c) and rate of deformation (d) of spring. | 33 |
| Figure 29. Power comparison between input and output power. Simulation (left) and experiment (right)..... | 34 |

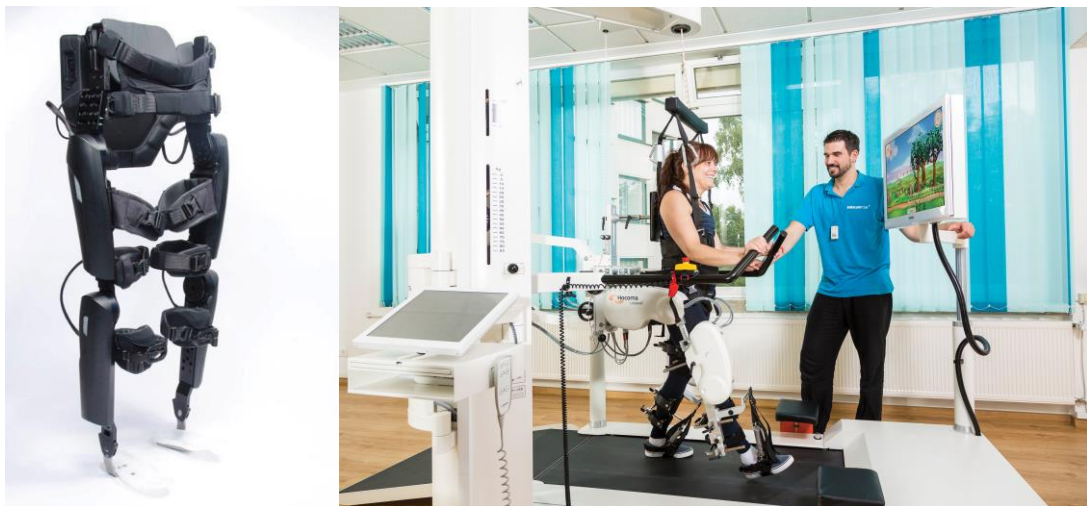
1.0 Introduction

1.1 Background and Motivation

Wearable devices in the medical field have been used for over a century to assist the motor functions of an impaired limb [1]. The most basic devices were passive devices, composed of metal bars and leather straps intended to aid a person to perform daily tasks that has become arduous or even impossible due to decrease or absence of muscle function. Among those tasks, perhaps the most rudimentary to human desire was to restore the ability to walk.

Multi-joint lower limb devices assist the functions of pelvis, knee and ankle joints that control almost all aspects of gait. Currently, there are products in the market such as the Rewalk [2] and the Lokomat [3]. These have a series of actuators located near each joint and a power source either worn by the user or tethered to the ground. Depending on the purpose or design, these wearable devices can be categorized into two groups: rehabilitation or augmentation.

Rehabilitation wearables are intended to restore the weakened motor function and are used in a hospital or physical therapy environment. Wearable devices can be intended to augment the user to replace a lost motor function or provide additional power to surpass that of a human. These devices are typically intended for military or construction settings. The number of different types of lower limb wearable devices and the number of those commercially available indicate how much development is done around wearable devices that assist the pelvis, knee and ankle joints.



*Picture: Hocoma, Switzerland (right)

Figure 1. Multi-joint wearables in the market. The Rewalk Personal 6.0 (left) and Lokomat (right).

The scope of wearables extends to devices specific to a single joint such as an ankle-foot orthosis (AFO) that controls the motion of one joint. Among the different types of single-joint wearables, the AFO has been the interest of many researchers as the ankle plays a key role in the gait cycle, which will be discussed further in the next section.

An ankle-foot orthosis (AFO) is a device specific to the ankle joint that restricts its range of motion by controlling the stiffness [4]. Typically, eversion and inversion movements of the foot are held rigid and the range of motion in the sagittal plane is limited. By constraining the movement of the ankle to a certain range, it is able to stabilize the foot and control its position. A common condition that the AFO is prescribed to is foot drop, which is an abnormal gait pattern characterized by the inability to dorsiflex the ankle or raise the foot to give enough clearance for the leg to swing forward. AFOs are also used to give support to a weakened joint allowing it to bear more weight.

AFOs can be categorized into two main types: passive and powered AFOs. The majority of AFOs are passive devices that focus on restraining movement of the ankle rather than strengthening the muscles during gait. They are not able to add positive power during gait and can only utilize the energy stored from the natural movements of the body. Therefore, passive AFOs are used to treat a condition and alleviate the symptoms such as foot drop instead of being used for therapeutic purposes. Passive AFOs are made from a variety of materials including plastics, metals or carbon fiber. Many products are available commercially and easy to acquire.

Powered AFOs use an actuator and power source to provide positive power during gait. The ankle position can be controlled actively allowing a much more natural gait pattern. Similar to multi-joint wearables, powered AFOs are used for rehabilitation and augmentation purposes. Unlike passive devices, the muscle is stimulated during gait allowing regeneration of muscle function. Powered AFOs can be categorized according to different types of actuation such as electromechanical or hydraulic. Depending on its purpose, the capability of actuation can range from providing the entirety of power required by gait to only a portion assuming the rest can be provided by the user. A review of powered AFOs can be found in Section 1.5.



Figure 2. Hydraulic Ankle-Foot Orthosis (HAFO) developed by University of Minnesota.

It has been the focus of research to design an AFO that provides the power demanded of a normal gait and some have achieved it using different methods of actuation [1]. However, it is equally important for an AFO to be lightweight, compact and safe. It is a challenge to achieve both the power required by gait and a lightweight system. A large portion of the weight comes from the actuator and power supply which is inevitably heavy and bulky due to the high power required during gait. Current designs output a portion of the gait power or use a large power supply tethered to the ground or worn as a backpack. However, a study shows how oxygen intake, which is an indicator of metabolic rate, increases as the weight of the device located at the ankle is increased [5]. Considering the technology used to design an AFO can be extended to many applications such as orthoses for other joints in the body or even as part of a multi-joint wearable system, the task of designing a lightweight, portable and safe actuator is paramount to the advancement of wearable technology.

1.2 Ankle Dynamics of Human Gait

In designing the actuator for an AFO, it is important to understand the dynamics of an ankle during normal gait. Gait is the repetitive movement and torque of the pelvis, knee and ankle joints that occurs when a person walks. Figure 3 illustrates the progression of one gait cycle as it starts with one foot hitting the ground, ‘heel strike’, and ends when the same foot reaches its second heel strike. There are intermediate positions that characterize stages in the cycle. After the initial

heel strike, the foot stays on the ground until the ‘toe off’ position leading to the ‘mid swing’ position at which the foot is off the ground and swinging towards its next step.

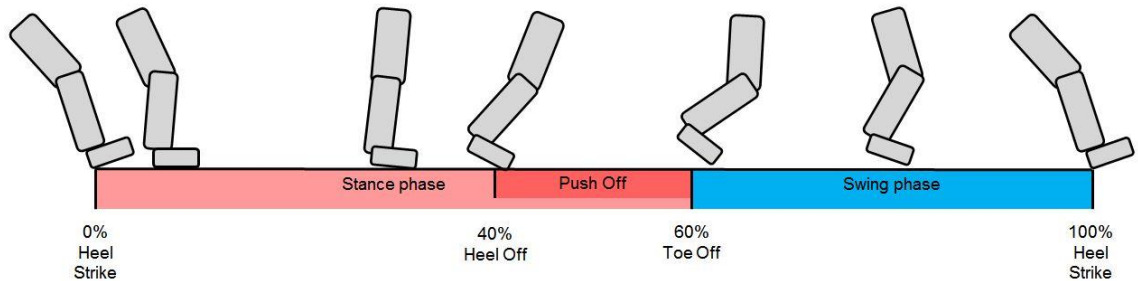


Figure 3. The human gait cycle.

Observing the kinematics and kinetics of the ankle joint gives better understanding of how the ankle is used to propel the body forward. For the purpose of designing an AFO with one degree of freedom, it is possible to consider simply the angular position and torque in only the sagittal plane. For the scope of this research, the average gait of a 56 kg male walking in a pace of 1 cycle/second is used. Figure 4 shows the kinematics and kinetics of the ankle [6]. The peak torque occurs at approximately 55% of the cycle just before the peak velocity is reached followed immediately by toe off. This portion of gait is of particular interest as it is when the peak power of 250W is required. Ordinarily, the actuator is chosen to encompass the whole range of angular velocity and torque required by gait which is heavy and bulky to be attached to an ankle. However, in figure 4 note how the average power is much lower than the peak power, which implies the power supply designed to target the peak power will not be used to its full capacity during the majority of the gait cycle. This high-peak and low-average power property of ankle makes it an ideal circumstance for using some type of energy storage component. In such a case, it is possible to store energy and release it to meet the demands of a high peak power, thus being able to design a power supply that is more efficient and lightweight.

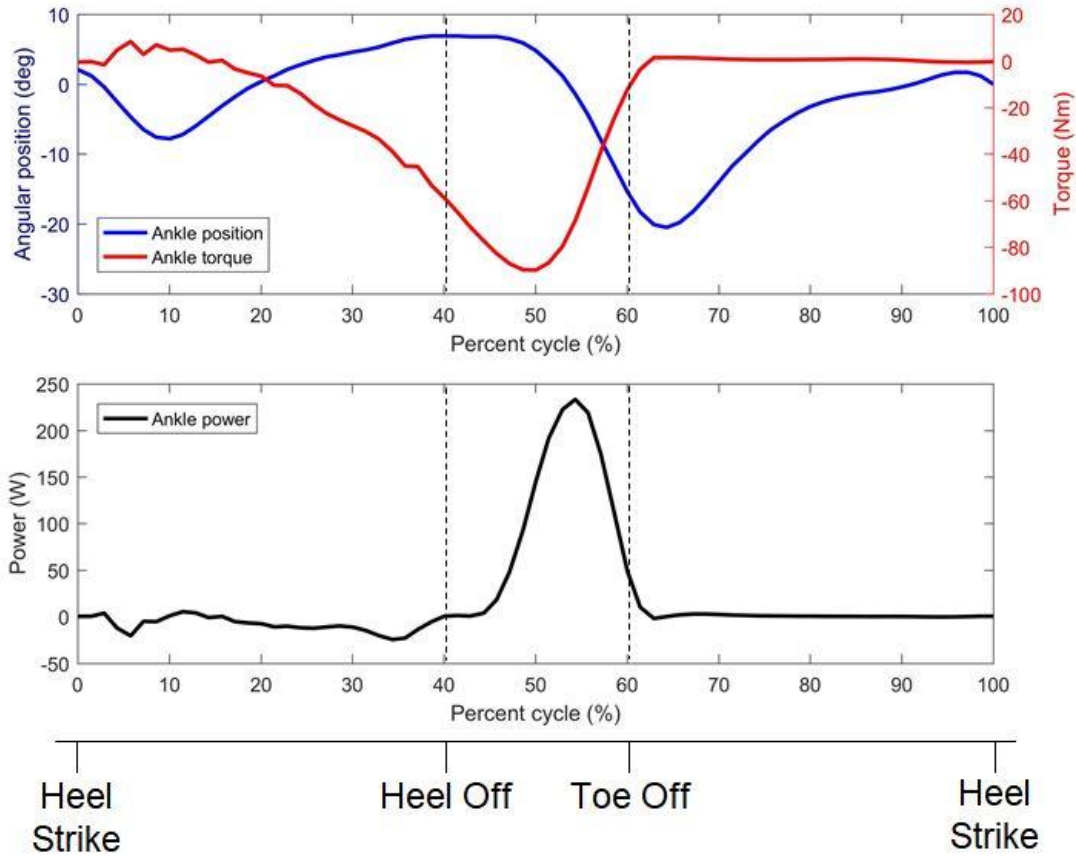


Figure 4. The kinematics and kinetics of the human gait cycle [5].

1.3 Series Elastic Actuators (SEA)

One method of energy storage is to use a series elastic actuator (SEA), which has an elastic element attached in series to an actuator. A spring attached to the end of a linear actuator is a typical configuration as illustrated in Figure 5. The SEA, introduced by Pratt in 1995, steers away from the conventional idea that a stiffer system is easier to control [7]. The term wearable entails the need for the device to be user-friendly, safe and lightweight for portability. The compliant element of a SEA is able to absorb any external impact from the user or environment reducing the damage to both the device and the user. More importantly and the aspect at which this research focused on, energy can be stored in the elastic element and later released to increase the peak power output. The peak power required at the ankle joint is high while the average is only a small fraction of that value. By choosing the correct elastic constant, the torque and velocity output from a power supply can be amplified to meet the requirements of a high peak power.

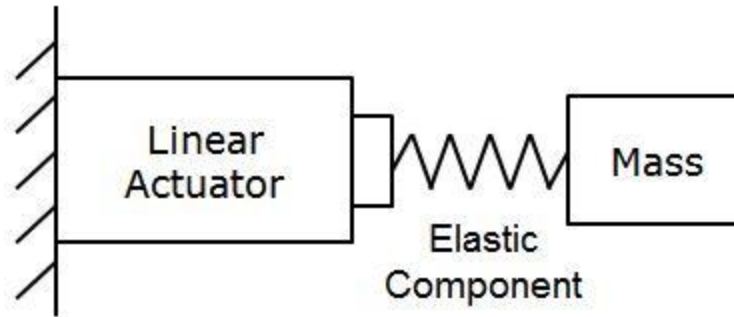


Figure 5. Components of a series elastic actuator.

1.4 Hydraulic Power

Hydraulic technology is common in heavy equipment used in construction but recent studies show promise in its application to wearable technology [8]. A hydraulic system has potential to lower the weight of the overall system while satisfying the power requirements of gait. While taking advantage of the inherent excellent power density of hydraulic systems, it is possible for the power supply to be separated from the actuator using hoses allowing it to be located away from the ankle. Recent research shows small scale hydraulics is efficient and lightweight compared to an electromechanical system above operating pressure of 500 psi [9]. The Hydraulic Ankle-Foot Orthosis (HAFO) developed by Human/Machine Design Lab at the University of Minnesota utilizes the advantages of a hydraulic system to make a compact and lightweight untethered AFO with a power supply located at the waist.

1.5 Prior art

Powered AFOs are not available commercially and instead exist in research facilities and universities. In 2004, the Massachusetts Institute of Technology (MIT) developed an AFO by attaching a series elastic actuator to a passive AFO [10]. (Figure 6) The series elastic actuator was used to actively change the compliance of the AFO during swing phase of gait. The main function of this AFO was to control the plantar flexion of the foot to avoid collision of the foot during swing phase. This does not require the AFO to provide high amounts of power as its main purpose is not to propel the body forward. It is similar to the goals of this study in its application of series elastic actuators to an AFO.

In 2005, the University of Michigan developed a lightweight AFO that provides plantar flexion and dorsi flexion assistance during gait [11]. (Figure 6) The AFO was intended for rehabilitation of neurologically impaired subjects either on ground or on treadmill. The form of actuation used

in this AFO is a pneumatic muscle actuator (PMA) which is an expandable bladder that is pressurized to provide unidirectional force. The actuator is back drivable and is located at the front and back of the AFO. Their design was able to output a force of 70 Nm during plantar flexion and demonstrated that a lightweight powered AFO using PMA was feasible. However, the PMAs have an inherent bandwidth limitation that makes them unfavorable when trying to control the exact position of the ankle. The weight of the AFO was 1.6 kg but was tethered to a remote power source.



Figure 6. AFO using SEA by MIT (left) and powered AFO using PMA by University of Michigan (right).

In 2011, a powered AFO using robotic tendon technology was developed by the Arizona State University and Washington University, St Louis [12]. (Figure 7) A robotic tendon actuator is a DC motor coupled to a lead screw in series with a spring. The actuator is located at the rear end and provides both movements in both directions of the sagittal plane. The AFO is aimed to provide 50% gait assistance which implies the AFO is able to produce the angular velocity of the ankle and provide 50% of the torque required. The actuator for this robot weighs 0.95 kg and is an example of how the peak power required for gait can be achieved using a smaller motor and a spring attached in series.



Figure 7. Powered AFO using robotic tendon technology.

1.6 Project Objective

The objective of this project was to understand whether a SEA would lower the weight of the HAFO. Designing a direct drive HAFO capable of producing the gait power requires a heavy power supply. However, by using a SEA, it is possible to reduce the weight of the power supply by storing and releasing energy, similar to how the body uses its tendons. Additionally, hydraulic technology allows the power supply to be separated from the actuator using hoses thus, minimizing the weight at the ankle. By combining the advantages of SEAs and hydraulic technology, it should be possible to design a lightweight AFO with a high weight to power output ratio.

2.0 HAFO Design using SEA

2.1 Direct Drive HAFO Design

A direct drive version of the HAFO was developed by Neubauer and Durfee from the Human/Machine Design Laboratory of University of Minnesota [13]. The design requirements were based on anthropic data and aimed to generate the necessary angular velocity and torque required during gait. The maximum allowable weight of the system was another requirement. It had an untethered power supply located at the waist to minimize the weight of the device at the ankle. A summary of the design requirements are shown in Table 1.

Table 1. Design requirements of direct drive HAFO

| | | |
|----------------------------------|----------------|--------|
| Maximum torque | Plantarflexion | 90 Nm |
| | Dorsiflexion | 10 Nm |
| Range of Motion (ROM) | Plantarflexion | 50 deg |
| | Dorsiflexion | 20 deg |
| Maximum angular velocity | 250 deg/sec | |
| Weight of device at ankle | < 1.2 kg | |
| Total weight | < 3.5 kg | |

The power supply is design as a closed-loop fluid power circuit with a bi-directional axial pump driven by a motor. The pump supplies fluid to the ankle at which two cylinders are located on each side of the ankle. A novel piston-cable hydraulic cylinder (PCHC) design, which uses a cable in place of a rod, was used to convert the linear motion of the actuators into rotational motion via a pulley. Because the cables were not able to push and rotate the pulley, cylinders were arranged in a pull-pull configuration connected to the pulley. The pulley is attached to a foot plate that constrains the position and delivers power to the foot. Figure 8 shows a rendering of the HAFO and its components.

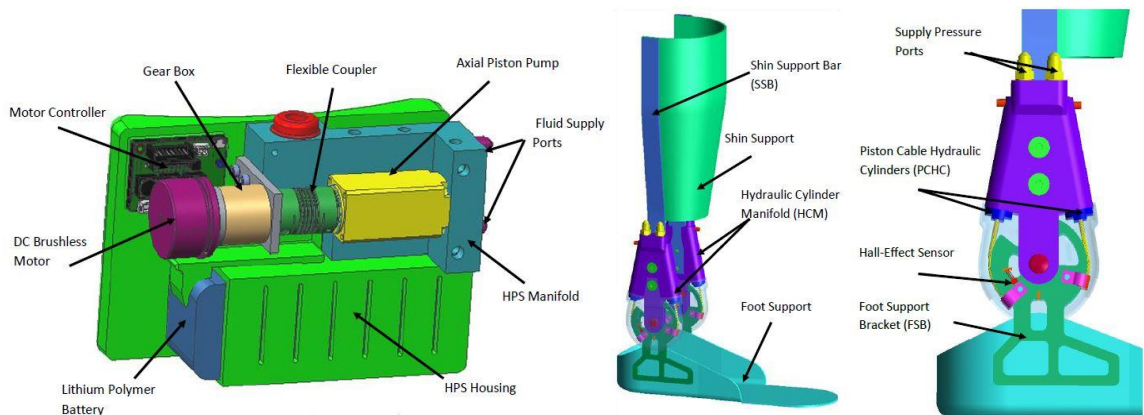


Figure 8. Direct drive HAFO. Hydraulic power supply located at the waist (left) and actuator at ankle (right).

Analysis of the maximum output torque and angular velocity showed that the direct drive HAFO was not able to meet both the torque and angular velocity requirements of gait. In other words, the HAFO would be able to assist the ankle movement but the user would have to depend on his or her own strength to support the body weight, not on the HAFO to provide the power required

to walk. In selecting the components for the power supply, the weight of each component had to be considered to meet the overall weight requirement of the system. A trade-off exists between the rated power of the motor and its weight. In the process, a brushless DC motor rated at 70W was chosen as the motor, coupled to a gear box with a reduction ratio of 3.7.

Although the direct drive HAFO can serve as a rehabilitation device, increasing the power output can widen the range of its applications. This research attempted to increase the power output of the HAFO by applying a SEA with little or no increase in its weight.

2.2 Designing a Hydraulic SEA

2.2.1 Comparison of different elastic components

An electromechanical system such as a ball screw driven by a motor can only use springs as its elastic component. In designing a series elastic actuator for a hydraulic system, different elastic components can be used to store energy, including a hydraulic accumulator which is the hydraulic equivalent to a spring.

Similar to springs in a mechanical system, accumulators are used to store energy and absorb shocks or external impacts to the system. Accumulators have the advantage of transferring power through fluid flow thus, being able to separate the energy storage component from the actuator similar to how the power supply can be separated through hoses. Another benefit of using an accumulator is the ability to isolate the energy storage component using an on/off valve placed in the hydraulic circuit. Despite the power amplification that a SEA can achieve, it is beneficial to have the ability to disengage the series elastic component. In the scope of this study, only the normal gait pattern is considered. However, future work involves different patterns of movement such as walking up a flight of stairs or even movement that does not occur in a cyclic repetitive pattern in which controlling when the stored energy is released may be important.

As an initial design process, three system architectures were considered to find the most effective way to store energy. All three had a linear actuator with a limited stroke and had identical bandwidth capabilities. The actuator and elastic components were assumed to be ideal and losses were ignored. The actuator commands the force applied to the mass which determines the velocity. The actuator accelerates a mass over the distance of the stroke was observed. The model of how energy is delivered to the mass was inspired by a past study done by Paluska and Herr [14]. In their study, they compared two electromechanical systems with and without a series elastic component. Additionally, a third system was added using an accumulator as the elastic component for this study. Figure 9 illustrates the three different systems.

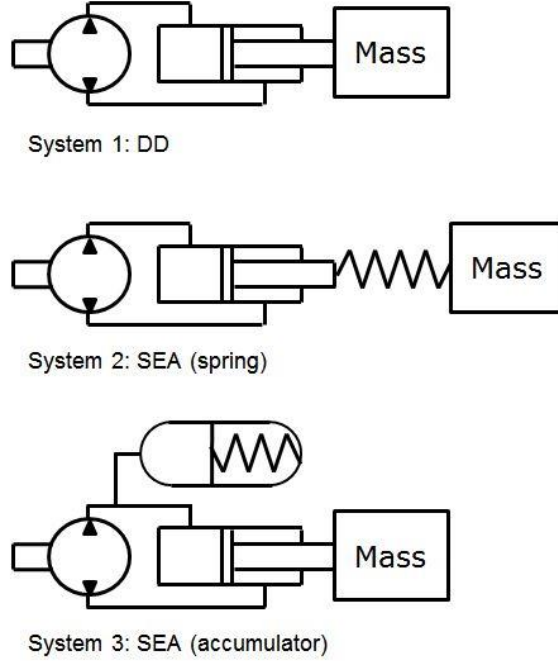


Figure 9. Configurations of the systems simulated. All configurations are closed-circuit hydraulic systems. System 1 (top): Direct drive, System 2 (middle): Series elastic actuator with spring, System 3 (bottom): Series elastic actuator with accumulator

Assuming the motor operates at its maximum power at all times, it delivers a force to the mass which decreases proportional to the velocity which is equivalent to a motor in series with a damping constant, $b = F_{max}/V_{max}$. System 1 was governed by the following differential equation.

$$m\ddot{x} = F_{max} - b\dot{x}$$

In system 2, a spring with elastic constant, k_{spring} , was attached in series to the actuator. The actuator has the same maximum force and damping constant that governs the velocity under load. The differential equations that characterize the system become a second order system and were derived as below.

$$\begin{aligned}\Delta x &= x_{mass} - x_{actuator} \\ F_{max} - b\dot{x}_{actuator} &= -k_{spring}\Delta x \\ m\dot{v}_{mass} &= -k_{spring}\Delta x \\ v_{mass} &= \dot{x}_{mass}\end{aligned}$$

Deriving the transfer function with the velocity of the mass as the state variable gave:

$$\frac{v_{mass}}{F_{max}} = \frac{\frac{k_{spring}}{mb}}{s^2 + \frac{k_{spring}}{b}s + \frac{k}{m}} \quad (1)$$

In system 3, a spring loaded accumulator was used as its energy storage element. The actuator in this system was a hydraulic cylinder capable of providing the equivalent power as the other systems and assumed to be ideal. For a hydraulic system, the state equation was non-linear and the Simscape Hydraulics software was used to simulate the system [15]. State equation (1) is simulated using Matlab function *lsim* to validate the Simscape simulation matches the results from the derived equations. The spring constant was normalized by m/b^2 to put in dimensionless form. The same normalized spring constant was used for both SEA systems.

Figure 10 shows simulation results of the normalized velocity of the mass for each system when a constant voltage is supplied to the motor. The velocity of system 1 is that of a typical first order system. The rate at which velocity increased declined as velocity reached its maximum value. The two SEA systems were second order underdamped systems. The amount of velocity amplified was equivalent to that of power amplified since constant force was applied. There is a trade-off between power amplified and the bandwidth of the system. As the normalized spring constant increased, it approached the direct drive case. As the spring constant decreased, the power amplified increased but the speed of the system decreased.

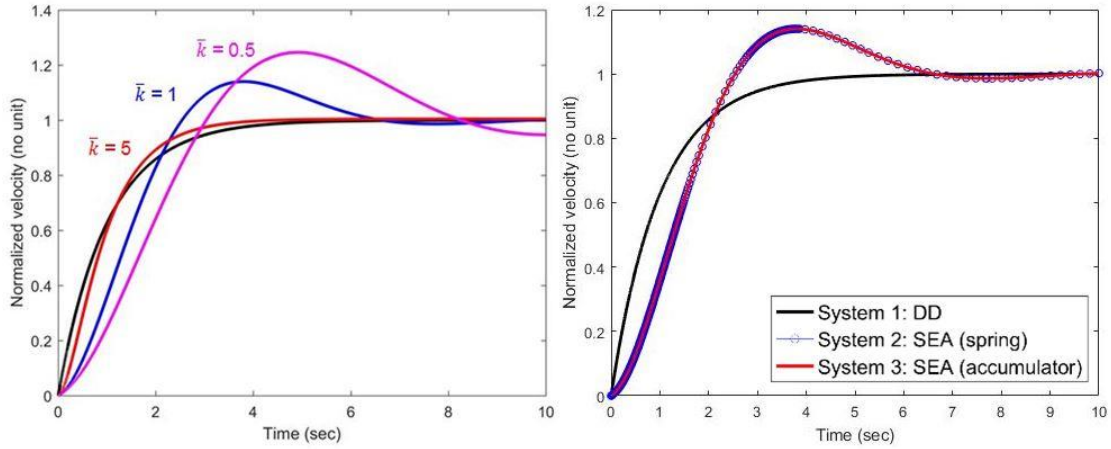


Figure 10. Normalized velocity of mass with different spring constants (left) and of the three different systems.(right)

When the normalized spring constant for both SEA systems were the same, the amount of velocity amplification was identical. The simulation results assumed no losses and ideal efficiencies thus it can be said that the elastic component with fewer losses has better power amplification capabilities. When the losses associated with a spring and an accumulator were compared, a spring had nearly no losses compared to an accumulator which had losses in the hoses used to deliver power. Furthermore, an accumulator was heavier than a spring. A type of lightweight accumulator is the diaphragm accumulator which is heavier than a spring given similar energy storage capabilities. The housing of the accumulator needs to contain the pressurized fluid is the main reason an accumulator is heavier than a spring. This comparison between different systems was necessary in understanding the feasibility of different elastic components. Therefore, despite the advantages a hydraulic accumulator had over a spring, the added weight of an accumulator and the inefficiencies due to conduit losses resulted in a spring as the most effective component to achieve series elasticity.

2.2.2 Spring Constant and Power Amplification

In designing a SEA, choosing an optimal spring constant is important. It directly related to how much power could be amplified and what the power requirements of the motor needed to be when choosing a power supply. Hollander et al. [12] developed an electromechanical powered ankle-foot orthosis using a motor and ball screw and a series spring. They derived an equation solving for the motor power requirement as a function of spring constant when the desired power was given. The desired power was the angular velocity and torque requirements of gait. The following derivation is from Hollander and the result was used to determine the spring constant.

A free body diagram of a SEA is shown in Figure 11.

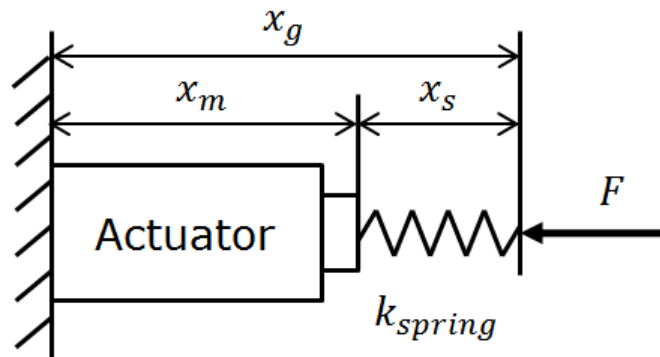


Figure 11. Model of series elastic actuator.

An advantage of SEA was that the force at the end point is directly proportional to the deformation of the spring.

$$F = k_{spring} \cdot \Delta x_{spring}$$

The position of the motor end point was solved relative to the distance between the spring end point and ground

$$x_m = x_g - x_s$$

The spring length was

$$\begin{aligned} \Delta x_{spring} &= x_0 - x_s \\ x_s &= x_0 - \frac{F}{K} \end{aligned}$$

Substituting the equation for the length of spring into the distance of the motor end point and taking the derivative gives the velocity of the motor in terms of the velocity of the spring end point and amount of spring deformation.

$$\dot{x}_m = \dot{x}_g + \frac{\dot{F}}{k_{spring}}$$

The power required by the motor was acquired by multiplying by the force seen during gait

$$P_{m,max} = \max \left| F \cdot \dot{x}_g + F \cdot \frac{\dot{F}}{k_{spring}} \right|$$

The first term on the right side is the power from gait which was summed with the power from the spring as a result of deformation. As the motor is the only source delivering power to the system, the value was always positive. The value of interest was the maximum power throughout the gait cycle as it gives the maximum possible value of power output by the motor. It is noteworthy that the parameters of this equation are all given values from the gait analysis data except for the spring constant. Consider a case with infinite spring constant, which is equivalent to an actuator without an elastic component. The power required by the motor is simply the power required by gait. When the spring constant reaches zero, it becomes an overly compliant system, which would require nearly infinite amount of power by the motor to output the power required by gait. From a calculation of the extreme spring constant values, it can be expected that there is an optimal spring constant that minimizes the power required by the motor.

Consider the angular velocity and torque required by the gait of an 80 kg male walking at a constant pace of 4km/hour. The peak power during gait occurs at approximately 55% of the gait cycle at 250W. Another design aspect was the transmission that occurs as rotational motion of the ankle is transformed to linear motion into the spring. A pulley was used to make this transition and the radius of the pulley affects the force and velocity values. As an initial analysis, a pulley radius of 30 mm was used.

Figure 12 illustrates the power required by motor as a function of spring constant. The trend leading to the infinite value of spring constant shows the motor power reaching the peak power required by gait. The motor power trends toward infinity as the spring constant goes to zero. The plot shows a relationship in which the power decreases below the peak power of gait at 20,000 N/m and reaches a minimum motor power of 95 W with a spring constant of 40,000 N/m. This suggests that any spring constant chosen that is greater than 20,000 N/m will require a motor power less than that of required by gait. When the optimal spring constant of 40,000 N/m is chosen, the power requirement of the motor is 40% of the gait power.

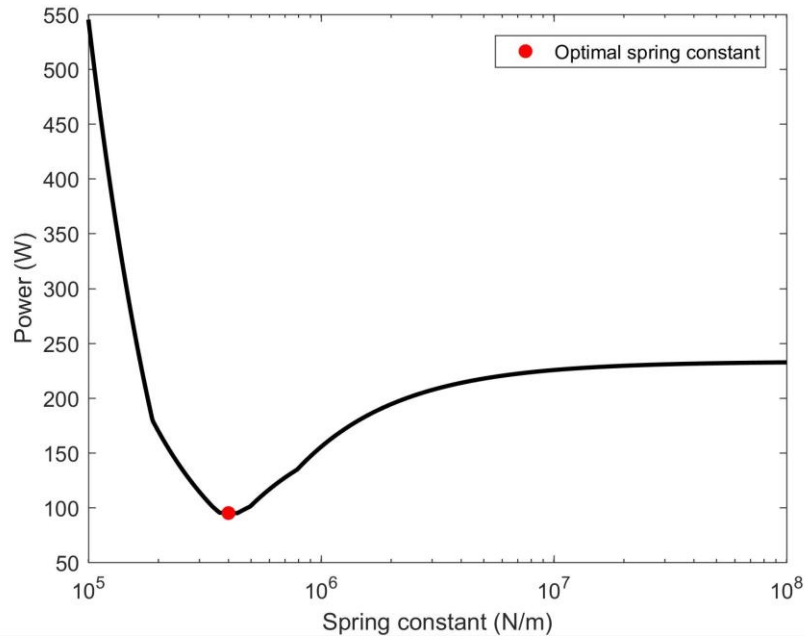


Figure 12. Optimization of spring constant by maximizing power amplification.

From the analysis, the spring constant was determined by two factors: the desired gait and pulley radius. The pulley radius is a key aspect of designing a compact AFO. Figure 13 shows the optimal spring constants as a function of the pulley radius. The spring constant decreases as the pulley becomes larger. However, the rate of decrease decreases as the pulley radius grows. The

spring size and weight is proportional to its spring constant, thus a trade-off exists between the size and weight of the pulley and those of the spring.

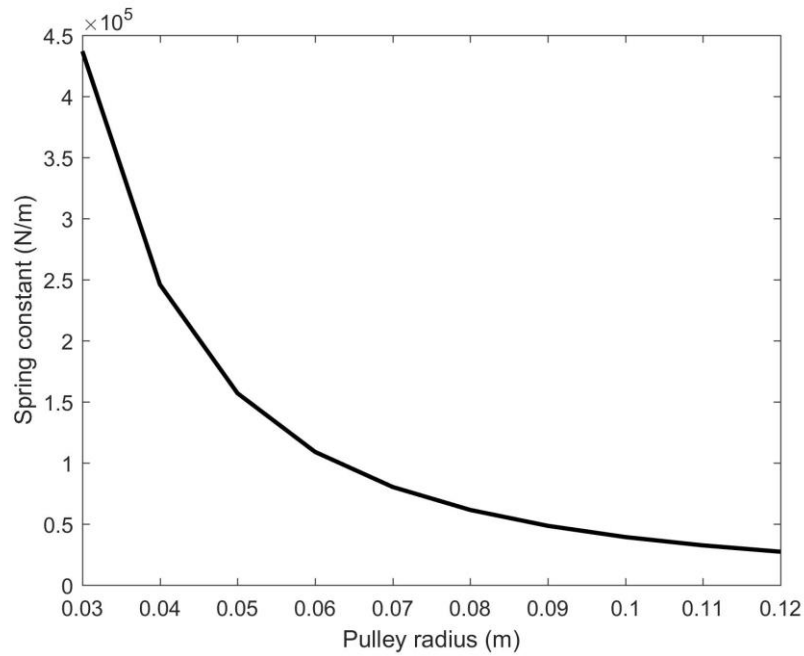


Figure 13. Spring constant versus pulley radius.

2.2.3 Gait Simulation

To verify the results of calculation, a model of HAFO using SEA was simulated using Simscape Hydraulics. To isolate the effect of the spring, three systems were compared: a 250W direct drive (DD) system, 95W DD model and a 95W SEA model. The velocity-torque limitation of the motor was based on the minimum power required and designed to be 95W. A PD controller was used to track the desired position of the ankle and the torque required was applied to the end of the spring. A diagram of the simulation is shown in figure 14.

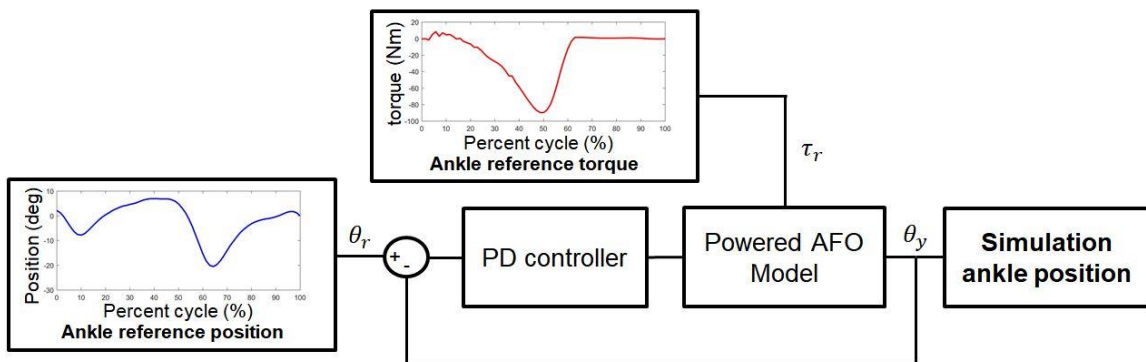


Figure 14. Block diagram of simulation. The ankle reference position and torque are identical to the data from Section 1.2 [6].

The powered AFO model in figure 14 is explained in detail in figure 15. The hydraulic circuit is closed and the bi-directional axial pump is connected to the rod end of each cylinder. A spring was connected in series to the rod of the cylinder. The power rating of the motor was determined by setting the no-load angular velocity and stall torque. The angular position of the pulley corresponded to the ankle joint and was measured to observe how well the reference position trajectory could be tracked. The torque required by the ankle is applied to the pulley. Figure 15 shows the series elastic actuator model. The direct drive model is identical with the exclusion of the spring.

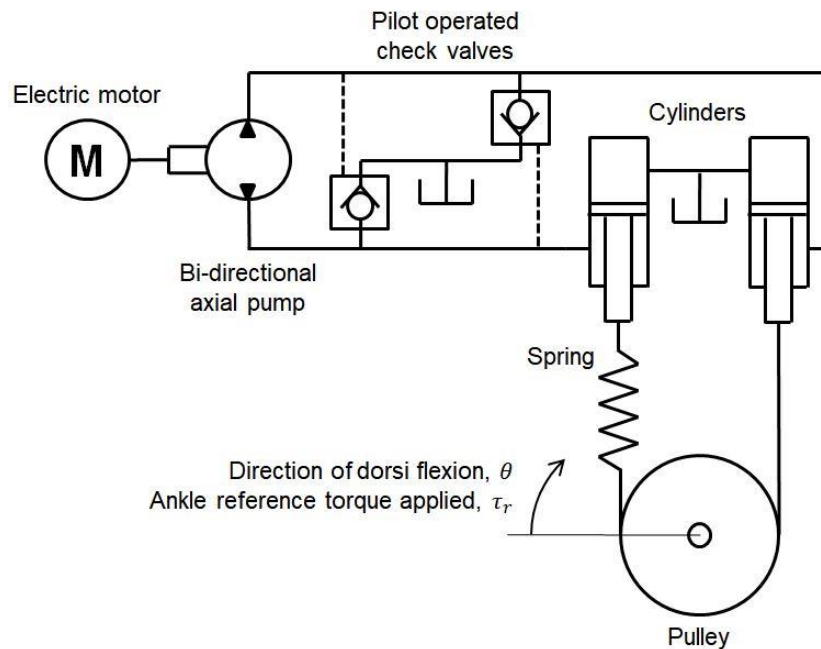


Figure 15. Model of powered AFO using SEA

DD System Simulation

A DD system of the HAFO was simulated to meet the demands of human gait. Two DD systems with different motor power ratings were compared to verify the simulation and to observe a case in which the motor is underpowered. A direct drive system must meet the peak power requirements of 250W. When a motor of 250W is paired with the appropriate transmission, it should be able to track the position of ankle during gait under load and was the base standard to which the performance and weight of SEA model was compared. Another DD model with an underpowered 95W motor was also simulated.

Figure 14 shows both models tracking the angular position of the ankle. The ankle reference position starts at heel strike and ends at the next heel strike. The first heel strike occurs at 0 seconds and the cycle ends at 1 seconds. The 250W model tracked the position well while the 95W system deviated from the desired position in the 0.5 to 0.8 second region. Consider a person walking with the aid of an underpowered AFO. The external torque applied is equivalent to the user's body weight bearing down onto the ankle. Without sufficient power the AFO is not able to withstand the user's weight to propel the user forward.

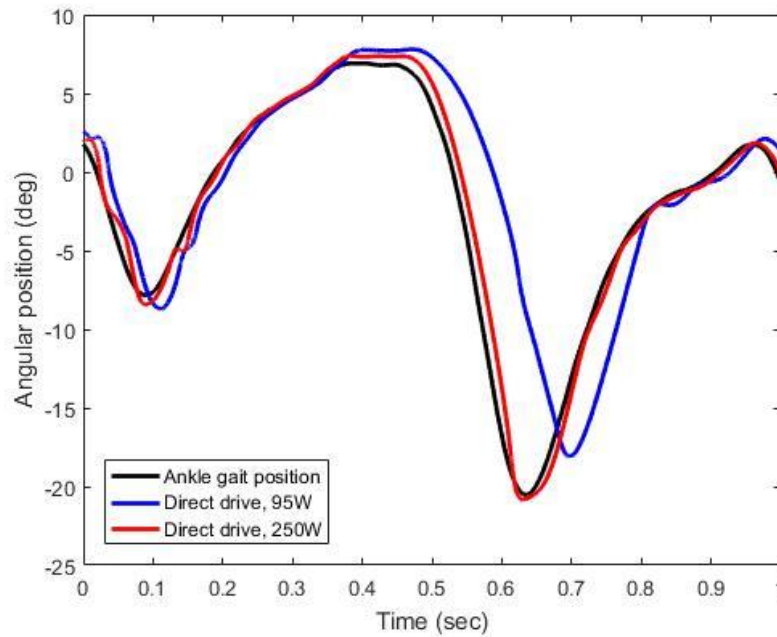


Figure 16. Position tracking of 95W and 250W direct drive systems during simulated gait.

Figure 15 illustrates the gait power was nearly met by the 250W motor direct drive system the 95W motor system was not able to generate enough power.

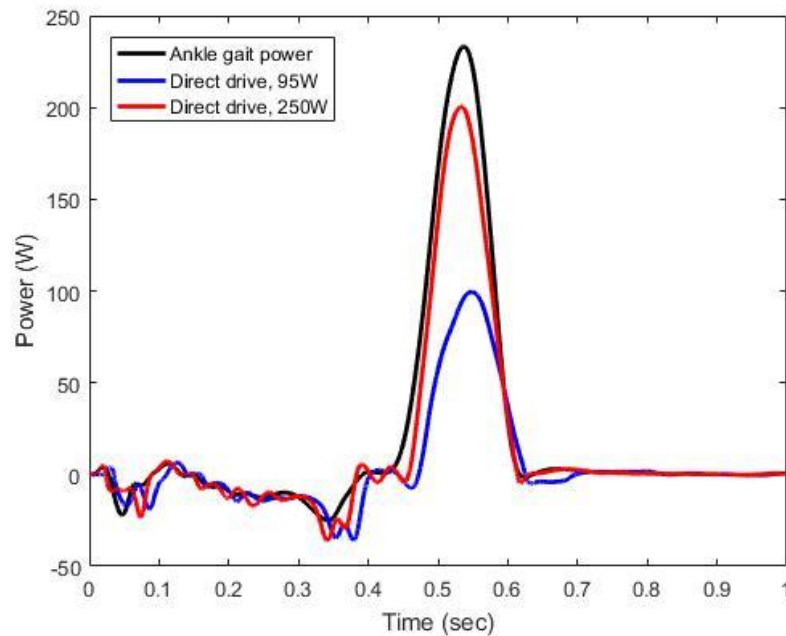


Figure 17. Power required by gait versus power generated by the DD systems.

SEA System Simulation

A SEA system was simulated to compare to the DD cases. The spring constant used in the simulation was 40,000 N/m as found from the method described in Section 2.2.2. The motor was the same as the 95W direct drive system. Figure 16 shows the ankle gait position tracked by the SEA. Compared to the direct drive case, the position was tracked better with a SEA system. The position of the ankle was able to follow the desired ankle position when is near its peak power. However, the actuator position, prior to when the energy is released, deviated from the desired position and some oscillation could be seen. One notable difference in controlling the position of a SEA was the commanded position was altered to account for the deformation of the spring [16]. However, this method has limitations as it required the torque of the ankle to be known in advance to determine the profile of ankle position.

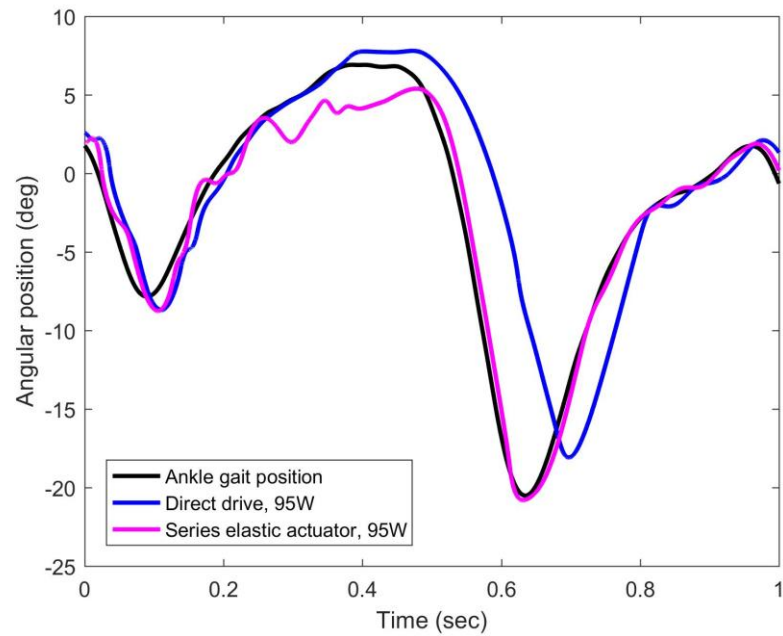


Figure 18. Ankle position tracking comparison of DD and SEA 95W systems.

The power profile of the SEA showed the power generated at the joint meets the demand of gait in Figure 17. The results verified the power amplification capability of applying a SEA. Compared to the DD scenario with the same 95W rated motor, the position was better followed and the peak power requirement was met by adding a spring with the appropriate elastic rate.

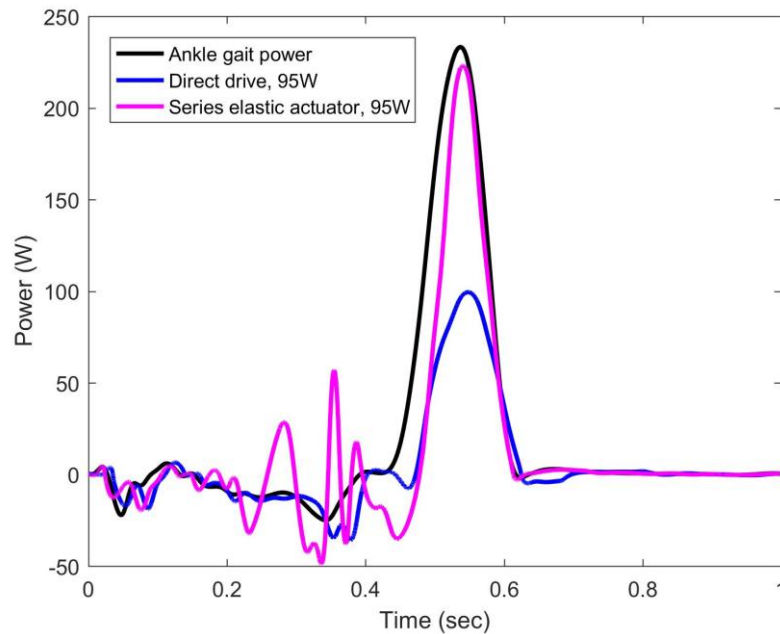


Figure 19. Power required by gait and power generated by DD and SEA.

2.3 Conceptual Design of a Hydraulic Series Elastic Actuator (HSEA)

2.3.1 Design Requirements

To implement the SEA into a HAFO design, several design requirements were established. The base requirement was the capability to produce 100% of the angular velocity and torque of gait. Given the HAFO was designed for a specific gait pattern used for the analysis, a motor with a rated power of 95W and a pulley radius of 40 mm was chosen. Since a trade-off exists between pulley radius and spring size, the largest pulley radius was chosen so the HAFO can fit inside a pant leg while minimizing the size of the spring. The spring constant appropriate for this pulley radius was 25,000 N/m. A similar piston-cable hydraulic cylinder design used in the direct drive HAFO was used to convert the linear motion into rotational motion.

Another design consideration was the ability to switch between direct drive and series elastic modes. The motivation behind using a SEA was to mimic how the human tendon stores and releases energy. Normal walking patterns are repetitive. The energy stored in the spring is released immediately to propel the body forward. However, irregular movements may require the ability to store energy and release it upon a precise desired timing.

Figure 23 shows a diagram of design requirements categorized by the demand to which each requirement satisfies. Each box represents a demand and the bullet points within are design requirements established to meet those demands.

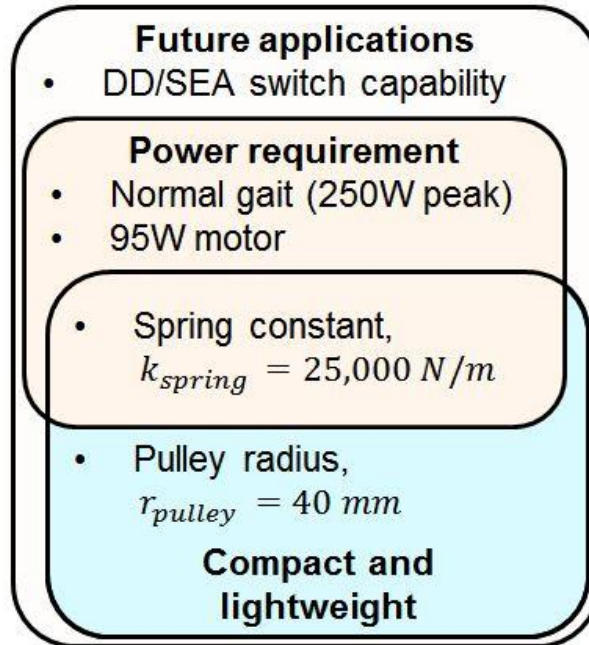


Figure 20. Diagram of design requirements categorized into specific demands.

2.3.2 Hydraulic Series Elastic Actuator (HSEA)

To incorporate a spring in series with a hydraulic cylinder, the simplest method would be to add a spring at the end of the cylinder rod. However, adding a spring to a piston-cable hydraulic cylinder is more complex as cables are flexible. As a solution, a double acting cylinder with three chambers and the spring located inside the cylinder was designed. The cross-section of the design is shown in Figure 24.

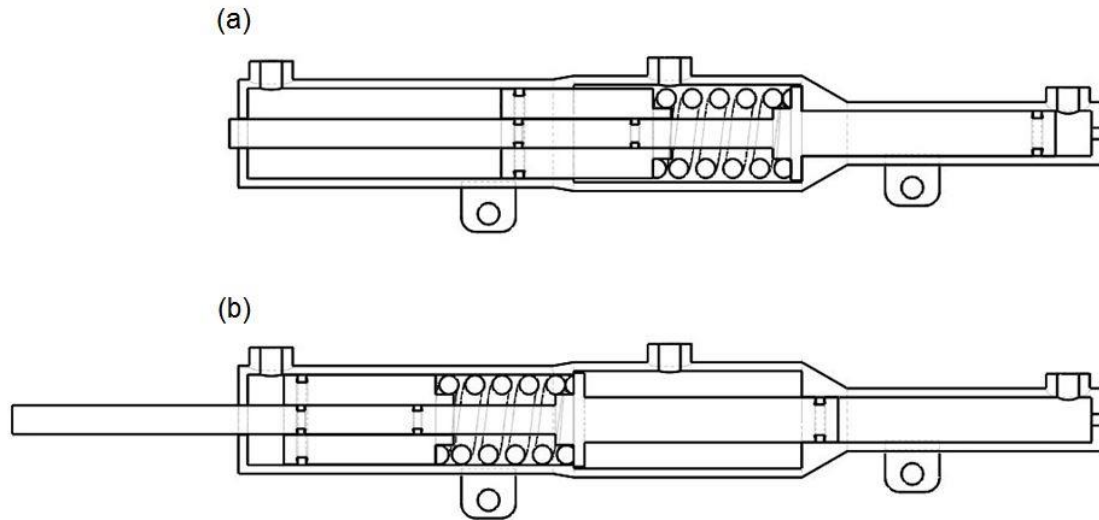


Figure 21. HSEA design in (a) retracted and (b) extended positions.

Figure 25 shows a simplified diagram of the HSEA. There are three ports allowing fluid in and out of the cylinder. Port 1 supplies the fluid for dorsiflexion and port 3 supplies the fluid for plantarflexion. Fluid flow into either port 1 or 3 of the cylinder pulls the cable which is connected to two pulleys. One pulley is connected to the joint allowing control of the ankle joint. The other pulley is idle. The series elastic component is in between the two pistons. By having the spring within the cylinder, it is possible to enable or disable the effects of the spring essentially acting as a clutch. When port 2 is open and fluid is allowed to flow freely in and out, the spring is enabled and the cylinder acts as a SEA. When port 2 is closed and the chamber is full of fluid, the incompressibility of fluid prevents the spring from deforming and acts as a DD system. When the port is closed when the spring is compressed, it allows the energy stored in the spring to be released at the precise desired moment to the advantage of the user.

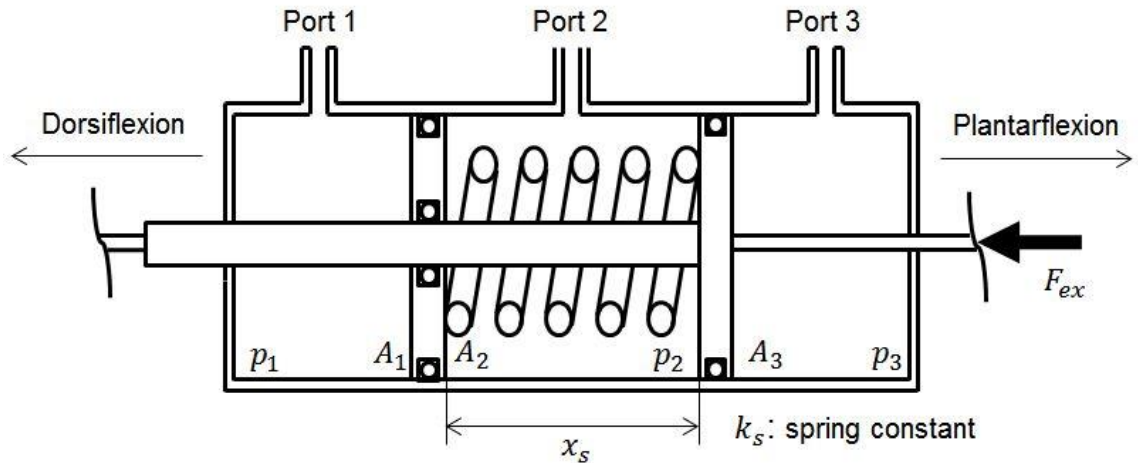


Figure 22. Simplified cross-section of HSEA and related parameters.

In SEA mode, fluid is allowed to flow out of the chamber into a reservoir allowing deformation in the spring. Consider the movements of the ankle that lead up to and during push off. The movements of the cylinder pistons are depicted in Figure 26. The direction in which the two pistons move relative to each other is important. As the ankle undergoes dorsi flexion, force is applied in the negative direction while the actuator applies force in the positive direction. This allows the spring to deform storing energy. Immediately as the ankle switches from dorsi flexion to plantar flexion, the energy in the spring is released in addition to the energy supplied by the actuator. At this moment, the cylinder is able to output a peak power greater than its rated power.

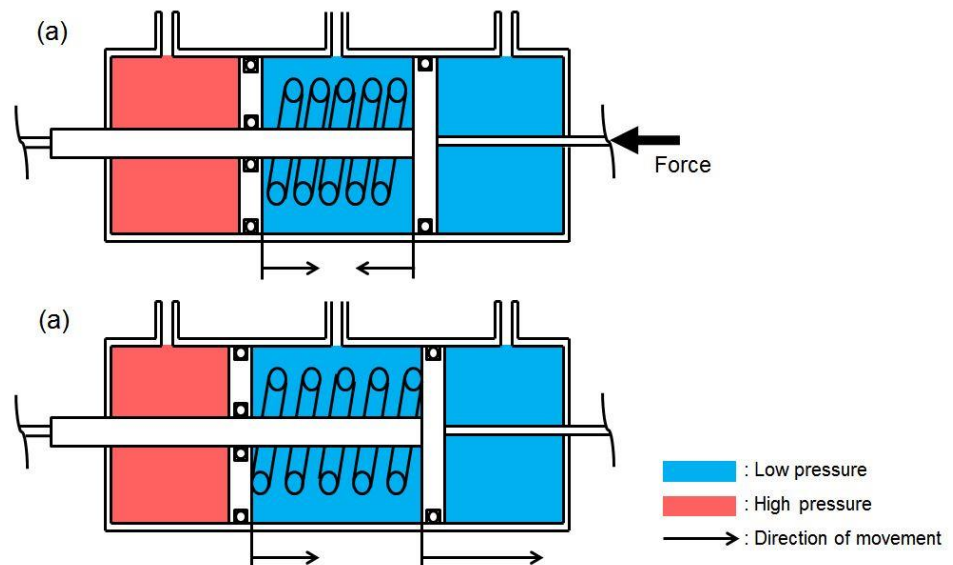


Figure 23. Cylinder piston movements during push off. (a) spring is compressed and (b) energy stored is released.

2.4 Weight Evaluation

The purpose of using a SEA with a hydraulic cylinder is to reduce the power required by the motor and ultimately to decrease the weight of the system. A component-wise analysis of several different actuation systems was done. Commercially available components were compared to explore a realistic solution. Additionally, the weight of the frame, brace and miscellaneous parts were not taken into account as the objective was to compare actuators. The components are chosen based on prior art. The first and fourth columns are existing AFOs that have been developed. The other components are chosen from the same manufacturer and series of products.

Five systems were compared. The first three systems were hydraulic systems. The direct drive HAFO developed by Neubauer and Durfee was a lightweight DD system [13]. However, it was not able to meet the entire demand of gait. The second system was also a hydraulic direct drive system. The difference between the two hydraulic systems was the rated power of the motor. The second system had a motor capable of meeting the gait power requirements but was heavier. The third hydraulic system was the SEA with a motor rating high enough to satisfy gait but has an additional spring component. The last two systems were both electromechanical (EM) systems. The first EM system was a direct drive SEA configuration developed by Hollander et al [12]. The fifth system was a direct drive system with the same performance. Table 2 summarizes the weight of each component in the five different systems.

Table 2. Component weight in kilograms of five systems

| Type | Hydraulic | | | EM | |
|-------------------------------|--------------------------|-----------------------|--------------------------|---------------------|--------------------|
| Configuration/ Performance | DD / Low | DD / Full | SEA / Full | SEA / Full | DD / Full |
| Motor | 0.14 Maxon EC 45 f | 1.1 Maxon EC 45 | 0.47 Maxon EC 60 f | 0.34 Maxon RE 35 | 1.1 Maxon EC 45 |
| Gearbox | 0.11 | 0.26 | 0.26 | 0.11 | 0.26 |
| Axial pump | 0.27 Takako 0.4 cc | 0.27 Takako 0.4 cc | 0.27 Takako 0.4 cc | - | - |
| Power supply manifold | 0.51 | 0.51 | 0.51 | - | - |
| Cylinder(s) | 0.35 | 0.35 | 0.35 | - | - |
| Spring(s) | - | - | 0.06 LHP207L04S | 0.05 | - |
| Lead screw | - | - | - | 0.45 | 0.45 |
| Total | 1.38 | 2.49 | 1.92 | 0.95 | 1.81 |

The bar graph (Figure 27) shows how the overall weight of each system is distributed between the ankle and the waist. All hydraulic systems were lighter at the ankle because the power supply is separated by hoses and located at the waist. The ankle weight is important because research shows that oxygen consumption increases when weight is The full-performance SEA hydraulic system, highlighted in red, had a lighter weight at the waist than the DD hydraulic system.

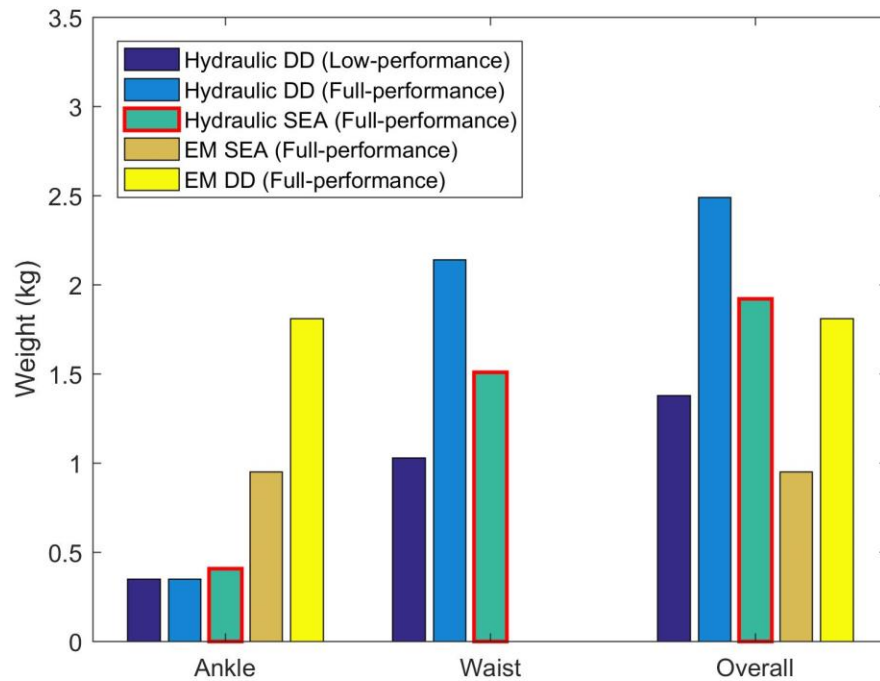


Figure 24. Weight distribution of different systems between ankle and waist.

3.0 Discussion

The application of SEA to a HAFO shows promise in reducing the overall weight while meeting the power requirements of gait. Different elastic components and the method selecting the elastic constant were explored. The model was simulated and showed the high peak power requirement of gait was able to be met by a lighter power supply compared to a DD model. Additionally, a HSEA design, capable of switching between SEA and DD modes, was proposed.

The HSEA design remains at a concept level. The next step is designing the details and prototyping the design to test its feasibility. It remains a challenge to design a relatively low power hydraulic system with commercially available parts. Another area that requires future work

is the control method of operating the HSEA. Dynamic control methods applied to SEAs have been explored by universities and research groups and can be applied to this technology.

In the future, a powered AFO will become an extensive device used not only for rehabilitation but for strengthening the human ankle to surpass human capabilities. The HSEA design with its increased power output and clutch capability opens up possibilities of exploring gait patterns other than normal walking. The technology extends beyond AFOs and can be applied to orthoses for other joints or even exoskeleton systems that combines multiple HSEAs.

References

- [1] Herr Hugh. (2009). Exoskeletons and orthoses: Classification, design challenges and future directions. *Journal of NeuroEngineering and Rehabilitation*, 6(1), 21.
- [2] ReWalk: More Than Walking. (n.d.). Retrieved August 15, 2017, from <http://rewalk.com/rewalk-personal-3/>
- [3] (n.d.). Retrieved August 15, 2017, from <https://www.hocoma.com/us/media-center/media-images/lokomat/>
- [4] Shurr, D., & Cook, T. (2001). *Prosthetics and orthotics* (2nd ed.). Upper Saddle River, NJ: Prentice Hall.
- [5] Pourghasem, Takamjani, Karimi, Kamali, Jannesari, & Salafian. (2016). The effect of a powered ankle foot orthosis on walking in a stroke subject: A case study. *Journal of Physical Therapy Science*, 28(11), 3236-3240.
- [6] Winter, D. (1990). *Biomechanics and motor control of human movement* (2nd ed.). New York: Wiley.
- [7] Pratt, G., & Williamson, M. (1995). Series elastic actuators. *Intelligent Robots and Systems 95. 'Human Robot Interaction and Cooperative Robots', Proceedings. 1995 IEEE/RSJ International Conference on*, 1, 399-406.
- [8] Center for Occupational Research Development, & United States. Department of Education. (1981). *Fluid Power Systems*.
- [9] Durfee, W., Xia, J., & Hsiao-Wecksler, E. (2011). Tiny hydraulics for powered orthotics. *Rehabilitation Robotics (ICORR), 2011 IEEE International Conference on*, 2011, 1-6.
- [10] Blaya, J., & Herr, H. (2004). Adaptive control of a variable-impedance ankle-foot orthosis to assist drop-foot gait. *Neural Systems and Rehabilitation Engineering, IEEE Transactions on*, 12(1), 24-31.
- [11] Ferris, D., Czerniecki, J., & Hannaford, B. (2005). An ankle-foot orthosis powered by artificial pneumatic muscles. *Journal of Applied Biomechanics*, 21(2), 189-97.
- [12] Hollander, Kevin W., Ilg, Robert, Sugar, Thomas G., & Herring, Donald. (2006). An efficient robotic tendon for gait assistance.(Technical Briefs)(Author abstract). *Journal of Biomechanical Engineering*, 128(5), 788-791.
- [13] Neubauer, B., & Durfee, W. (2016). Preliminary design and engineering evaluation of a hydraulic ankle-foot orthosis. *Journal of Medical Devices, Transactions of the ASME*, 10(4), 1-9.
- [14] Paluska, & Herr. (2006). The effect of series elasticity on actuator power and work output: Implications for robotic and prosthetic joint design. *Robotics and Autonomous Systems*, 54(8), 667-673.
- [15] Durfee, W., Sun, Z., & Van de Ven, J. (2009). *Fluid Power System Dynamics*. Center for Compact and Efficient Fluid Power. doi:<http://www.me.umn.edu/~wkdurfee/projects/ccefp/fp-chapter/>

- [16] Hitt, Oymagil, Sugar, Hollander, Boehler, & Fleeger. (2007). Dynamically Controlled Ankle-Foot Orthosis (DCO) with Regenerative Kinetics: Incrementally Attaining User Portability. *Robotics and Automation, 2007 IEEE International Conference on*, 1541-1546.
- [17] Waters, & Mulroy. (1999). The energy expenditure of normal and pathologic gait. *Gait & Posture*, 9(3), 207-231.

Appendix

A. Preliminary Experimental Analysis of a Novel Hydraulic SEA Actuator

Objective of experiment

A preliminary bench test experiment was conducted to achieve two objectives. The first objective is to validate the ability of series elastic actuator to amplify peak power. The second objective is to validate the results from simulation. This experiment was designed to test the amount of power amplification when series elasticity is applied to a hydraulic actuator. The angular velocity and torque profiles of normal gait are complex. Therefore, a simplified angular velocity and torque profiles were applied to the series elastic hydraulic actuator to demonstrate the amount of power amplified by the series elastic actuator.

Apparatus

The experiment used two single-acting hydraulic cylinders (Bimba HL-093-DPY) with their rods connected by a compression spring (Leespring LC 135L 03 S). Figure 18 shows a cartoon of this novel actuator.

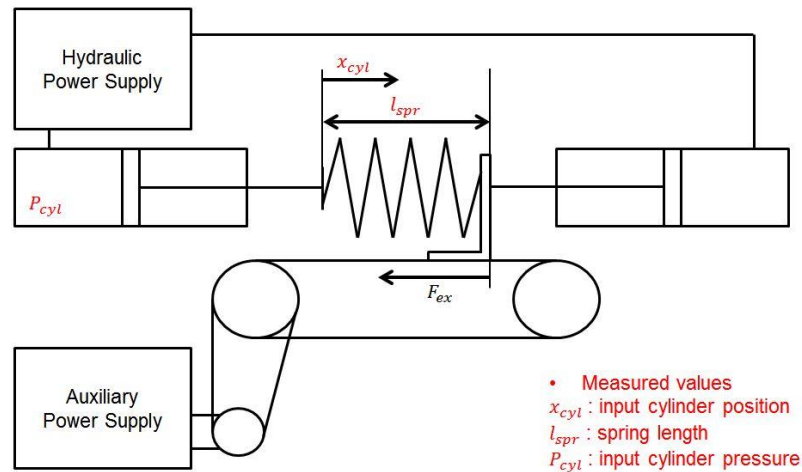


Figure 25. Apparatus.

There were two power supplies: the first power supply represents that of the HAFO and supplies the input fluid flow required to track the desired position and an auxiliary power supply that applies the external torque that is required to store energy into the spring. In gait, this external force is equivalent to a person applying their weight onto an ankle that leads to the propulsion of the body. A 70W rated motor (Maxon EC 45 flat) coupled with a 3.7:1 gearbox was used as the primary power source. The auxiliary source is a motor rated at 150W (Ampflow M26-150-P) with a system of pulleys with a 3.75 reduction ratio. Two motor drivers (Maxon 414533,

Roboclaw Solo 30A) are used to operate the motors separately. Pulleys and timing belts were used instead of lead screws to convert the rotational motion from the motor into linear motion as the transmission needs to be back drivable. To measure power amplification, the input and output powers were measured. Input power was measured as a product of force and velocity produced by the cylinder. Two linear potentiometers are used to measure the position of the input cylinder and deformation of the spring. A transducer (Omegadyne PX309-300A5V), capable of measuring pressure range 0 to 300 psi, is connected to the cap side of the input cylinder to measure the pressure and multiplied by the cap side area of the cylinder to solve for force. The amount of power amplified is measured by measuring the compression of the spring. Figure 19 shows a picture of the bench test setup.

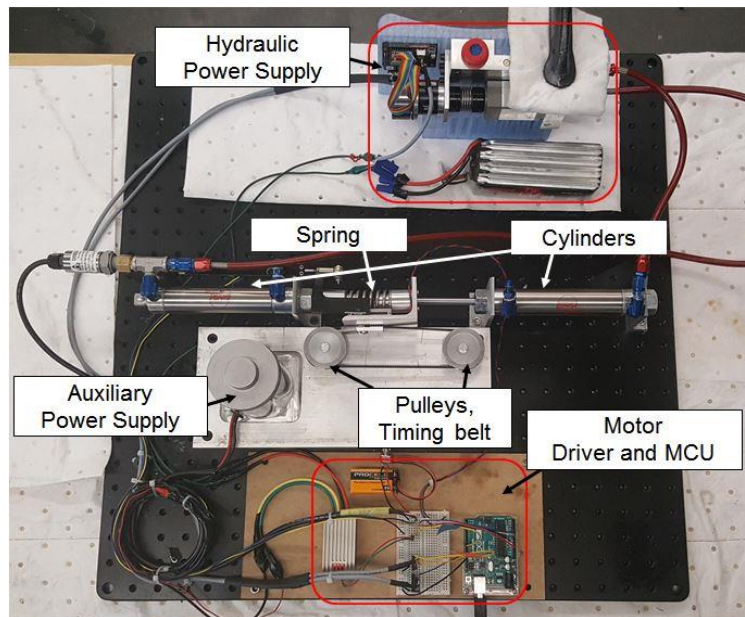


Figure 26. Series elastic actuator bench test setup.

The input cylinder was position controlled to move at a constant speed. An external force was applied via a secondary power supply to oppose the movement of the input cylinder. The same calculations used to select the optimal spring constant for gait is used with a solution of 20,000 N/mm. The spring constant used for the bench test was 18,660 N/mm, which is close enough to the optimal spring constant. Figure 20 illustrates the spring constant, 20,000 N/mm and minimum power required is chosen achieve a power of 21 W.

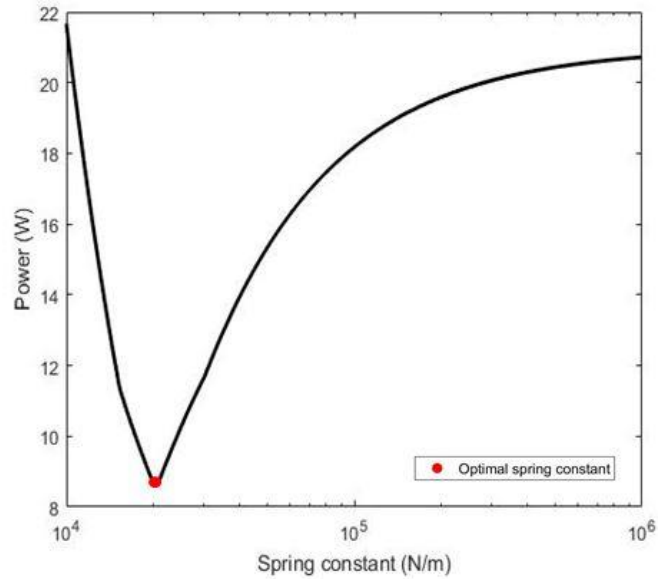


Figure 27. Selection of spring constant for bench test.

Results

Figure 21 shows the position and velocity of the input cylinder and spring end. The input cylinder refers to the cylinder to which power is delivered from the motor. The position of the input cylinder refers to the rod end respect to ground and was measured using a slide potentiometer. The end position of the spring attached in series was also measuring by a slide potentiometer. The motion of cylinder starts at 0.1 seconds and the constant opposing force is applied from 0.4 to 0.8 seconds during which the deformation of the spring shows the energy is being stored. The same oscillation during energy storage as in the SEA gait simulation was observed. At 0.8 seconds, the spring returns to its uncompressed length and greatly increased the velocity at the spring end.

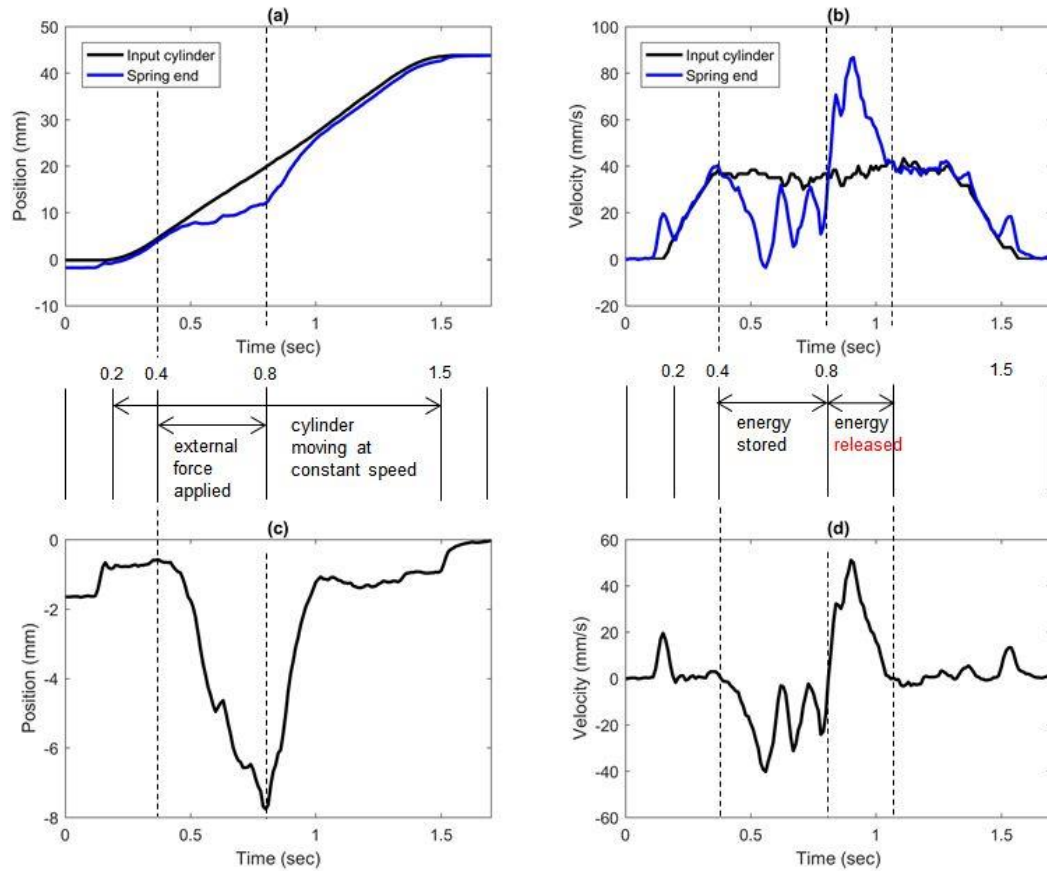


Figure 28. The position (a) and velocity (b) of input cylinder and spring end. The deformation (c) and rate of deformation (d) of spring.

Figure 22 directly compares the power generated by the cylinder and the power output when an external force was applied to the spring attached in series. The right figure shows the results from bench test. The power output at the spring end decreased between 0.4 and 0.8 seconds when external force is being applied but reaches its peak power at when the spring is uncompressed. The peak power of the SEA was 20 W with a motor input power of 8 W which was a 150% increase. The figure on the left shows the results from simulation. There is a discrepancy in the amount of amplification and peak power able to be achieved. First of all, the amplified peak power of the experiment was almost a 7 times higher than the simulation. The amount of amplification of the experiment was higher with 150% amplification compared to only 50% amplification of the simulation. However, in both cases the same kind of oscillation as in the gait simulation can be seen in both bench top experiment and simulation. The main reason I think there was such a discrepancy in results was because the motors were able to output more power

than the rated power. Also the voltage applied to the motors by the drivers were difficult to measure and as a result it was difficult to verify whether the same input is being applied to the motor in the experiment as the simulation. Validating the results from simulation is definitely an area that needs more work and one of the immediate steps to take.

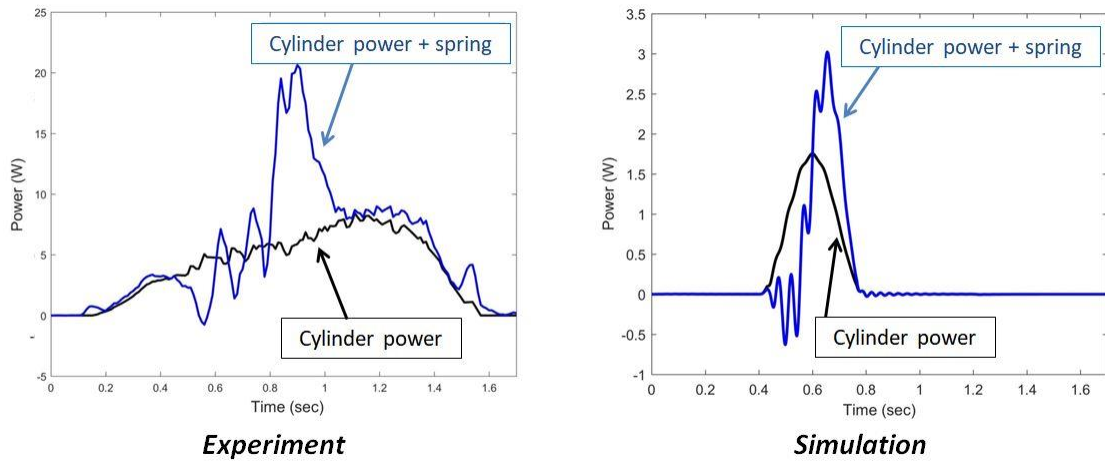


Figure 29. Power comparison between input and output power. Simulation (left) and experiment (right).